nature portfolio

Peer Review File

Surface hydrogen migration significantly promotes electroreduction of acetonitrile to ethylamine

Corresponding Author: Professor Liang Chen

This file contains all reviewer reports in order by version, followed by all author rebuttals in order by version.

Version 0:

Reviewer comments:

Reviewer #1

(Remarks to the Author)
In this work, Chen and co-workers describe the promoted electrosynthesis of ethylamine from acetonitrile using self-supported CuO@Cu heterostructure. By a series of characterizations and DFT calclulations, the authors confirm CuO serves as the catalytic site, with metallic Cu species significantly enhancing electron transfer. The migration of hydrogen atoms generated during the Volmer step to the adjacent site where acetonitrile is adsorbed is identified as the root cause of the enhanced acetonitrile reduction activity. Although the discussion about the valence of Cu in hydrogenation reaction is important, there are much fundamental issues about material characterization, electrochemical testing and theoretical calculations that need further discussion and data supplement:

1. The same materials and the same reaction have been reported by Jiao (Nat. Commun. 2021, 12, 1949) and Wang (Nat. Commun. 2023, 14, 3847) successively. The FE in this work is ~95%, which is roughly the same as previously reported (~94.6%, Nat. Commun. 2021, 12, 1949). So, compared with the above-mentioned catalytic system, I could not find the innovation and importance of this one and is only an addition to the field. What's more, the authors said, "... suggests a new strategy to enhance the electrochemical hydrogenation of organic molecules by regulating the Volume step". Questions like what happens to the other types of organic molecules by regulating the Volume step must be addressed.

2. The study demonstrates that the material comprises oxidized copper, as evidenced by a series of off-site characterizations. However, it should be noted that copper is highly susceptible to oxidation and phase transitions in an alkaline electrolyte environment. Consequently, off-site characterization could potentially result in misleading conclusions.

3. The reduction potential for the acetonitrile reduction reaction is found to be less than that required for the reduction of Cu2+ to metallic copper. This reaction process seems unreasonable and contradicts the test results given by Figure 1g that there is obviously a dissolution of Cu2O and electrochemical redeposition process in the electrochemical CV scanning. At such negative potentials or high current densities, can the Cu2+ in CuO@Cu stably exist? Or in fact, the real catalyst for the hydrogenation of nitriles is not the same as the CuO@Cu discussed in this work.

4. In an alkaline environment, the choice to utilize PEM instead of an anion exchange membrane (AEM) for flow cell experiments suggests a lack of profound insight into the fundamental principles of membrane electrode assembly devices on the part of the author.

5. In the stability test depicted in Figure 2, the pronounced selective fluctuation observed for ethylamine within the initial 100 hours is intriguing. Could this be attributed to alterations in the material's structural integrity? For 1H NMR tests, the author should provide internal standard curve of ethylamine. The author should describe the Faraday efficiency test method and producer in the stability test. In Figure S7, 1H NMR spectrum of the liquid products after 1000 hours test, peaks area belongs to ethylamine are significantly smaller than that of other samples, but the Faraday efficiency given in the text is still higher than 95%.

6. The authors contend that a synergistic interaction between Cu and Cu2+ is pivotal in the electrochemical hydrogenation of acetonitrile. Consequently, they propose the preparation and subsequent electrochemical evaluation of a range of Cu and Cu2+ compositions with varying proportions to elucidate this synergistic effect.
7. In-situ infrared spectroscopy conducted under open circuit potential (OCP) conditions may yield deceptive results, as Cu

is subject to phase transformations over time within a highly alkaline environment. Consequently, the adsorption data obtained may not accurately reflect the properties of the initial material. Furthermore, the authors have not thoroughly annotated the infrared absorption peaks, such as those at 1340 and 1180 cm-1, among others. In addition, the adsorption modes, such as adsorption via only the N atom or both the C and N atoms, of various molecules should be optimized and illustrated because different adsorption models lead to different shifts in FTIR. The simulated results should be compared with the experiment data to exactly determine the adsorption of the reaction species, hence a more accurate reaction mechanism.
8. On what basis is the model for the DFT calculations constructed? Analyzing the results reveals a discrepancy where the material contains a significantly higher proportion of Cu than Cu2+, yet the model inversely represents a greater abundance of Cu2+ over Cu. Models that are incongruent with experimental findings may yield deceptive outcomes. The vacuum layer in the Z direction is set to 12 Å, but considering that the authors placed more than 6 water molecules clusters as proton donors, a vacuum layer thickness greater than 15 Å is recommended.

9. In the DFT calculations, the authors postulate that the reduction of acetonitrile proceeds firstly via the Volmer step, involving the decomposition of H2O. The reader is left to ponder why the protons from water do not directly attach to the acetonitrile molecules, but instead are first dissociated onto the material's surface before being transferred to the acetonitrile for hydrogenation? During the hydrogenation of acetonitrile to ethylamine, the asymmetry of the acetonitrile molecule suggests the existence of multiple potential reaction pathways. The authors should meticulously evaluate these paths to identify the most favorable reaction trajectory.

Reviewer #2

(Remarks to the Author)
Tang et al. presented a CuO@Cu heterostructure catalyst with remarkable stability in the electroreduction of acetonitrile to ethylamine with negligible degradation over a 1000-hour test at a current density of 0.2 A cm-2. Detailed investigation on the catalytic mechanism have been performed and a synergistic hydrogenation process is proposed based on both experimental and theoretical evidence. Before acceptance, necessary revision is required.

1. The LSV curve of CuO@Cu heterostructure in 1 M NaOH solution should be given to demonstrate that the reduction of acetonitrile to ethylamine occurs more readily than hydrogen evolution.
2. The most important key point of this study was the improvement of stability. Do authors have any explanation on the remarkable stability?
3. A flow cell was assembled for the ARR test. I note that there is an activity enhancement after refreshing the electrolyte. Why?
4. The lattice fringes in HRTEM image (Figure 1e) are somehow unclear, please provide a clearer one, for example as an inset.
5. Water cluster was considered in the calculation of the barrier for hydrogen migration from solvent. Do the surrounding water molecules have any effect on the barriers for hydrogenation via surface adsorbed hydrogen?
6. Are the energies of the explicit water molecules included in the free energy profile? Are the energy change derived from CHE model comparable to that calculated in the kinetic calculation?
7. There are some typos in the manuscript, e.g., "Volume" in the Page 1 should be "Volmer". The quality of the figures could also be improved.

Reviewer #3

(Remarks to the Author)
The author constructed CuO@Cu Heterostructures were used to stabilize the electrocatalytic reduction of acetonitrile to ethylamine, showing good stability and Faraday efficiency. CuO was used as the active site, Cu enhanced electron transfer, and H* generated by Volmer step was transferred to the nearby acetonitrile to promote the reaction, which was verified by DFT. While the topic is of interest, there are several concerns and limitations that prevent the paper from being qualified for publicafion in Nature communicafions.

1.The author said that the formation of CuO and Cu heterostructure, but did not demonstrate in this paper.
2.The "Cu2 1O" in Figure 2b should be further defined as "Cu2+1O". What is the valence state of Cu in Cu2+1O? The red line is only described as Cu2O@Cu?
3.Acetonitrile can be reduced to 3-aminobutyronitrile, ethane (C2H6), NH3 and amines. What is the selectivity of producing ethylamine in this paper, and whether to produce other amine compounds.
4.The CuO shell on the catalyst surface, according to Fig. 3C, after 1000h of catalysis, the Cu0 valence peak is more obvious, while the Cu2+peak intensity decreases. Whether there is reconstruction during the reduction process (CuO→Cu).
5.The orange solid line in Figure 5b represents CuOx, but the specific valence state of Cu is not clear. As a comparison of the reaction path (CuO), the best reaction site and path should be given.
6.Does this electrocatalytic hydrogenation method apply to other nitriles?
7.In the references, the abbreviations and non abbreviations of magazine names are not unified, and references 5 and 24 are lacking. Reference 15 only gives the author's name, and other information is missing. Revise the non-conforming reference format of references according to the requirements of journals.
8.In the abstract and text, the abbreviation appearing for the first time should be marked with its full name.

Reviewer #4

(Remarks to the Author)
This manuscript reported a synergistic hydrogenation process for the electroreduction of acetonitrile, which involves both surface hydrogen migration and proton addition from solution. The hydrogen evolution could be terminated at the Volmer step, and the protons migrate to the unsaturated bond of acetonitrile over a CuO@Cu heterostructure, thus significantly promoting the acetonitrile reduction process. This is an interesting finding with the impressive performance. The as-prepared CuO@Cu heterostructure exhibited outstanding stability for 1000 h at a large current density of 0.2 A cm-2. I suggest its publication after suitable revisions.

1. The electroreduction reaction of acetonitrile to ethylamine has been investigated in 1M KOH solution only. How about the pH effect on ethylamine selectivity? For the long term stability test in figure 2e, Nafion 117 was used as the membrane to separate cathode and anode in the electrolyzer. Since Nafion 117 is a proton exchange membrane, how stable is it in alkaline condition? Have authors employed an anion-exchange membrane in their electrolyzer?
2. The authors claimed that there are Cu0, Cu+ and Cu2+ oxidation states in the simulated CuOx model according to the charge analysis. However, in Figure S13, only Cu+ exists in Cu2O (+0.53 |e|). Please comment on this.
3. In the computational details, authors indicated that the spin polarization was considered for CuOx. Is the spin effect significant for these Cu-containing systems? And The coordination enviorment and the side views of key reaction intermediates and transition states are highly suggested to be provided for reproduction.
4. The calibration curve should be provided for the reference electrode to prove the accuracy of the potential used in the study.
5. Cuprous oxide nanoparticles should be added as a control sample to compare with the CuO@Cu heterostructure for acetonitrile reduction.
6. An irrelevant horizontal line was observed in Figure 1. Please check and correct

Version 1:

Reviewer comments:

Reviewer #1

(Remarks to the Author)
The paper has been revised and now it is suitable for the publication.

Reviewer #2

(Remarks to the Author)
The authors have well addressed my concerns and I have no more comments on it.

Reviewer #3

(Remarks to the Author)
I agree with the revision, I think that can be published now.

Reviewer #4

(Remarks to the Author)
My concerns have been addressed largely. I recommend its acceptance.

Point-to-Point Responses to Reviewers' Comments and Suggestions

Reviewer #1 (Remarks to the Author):

In this work, Chen and co-workers describe the promoted electrosynthesis of ethylamine from acetonitrile using self-supported CuO@Cu heterostructure. By a series of characterizations and DFT calculations, the authors confirm CuO serves as the catalytic site, with metallic Cu species significantly enhancing electron transfer. The migration of hydrogen atoms generated during the Volmer step to the adjacent site where acetonitrile is adsorbed is identified as the root cause of the enhanced acetonitrile reduction activity. Although the discussion about the valence of Cu in hydrogenation reaction is important, there are much fundamental issues about material characterization, electrochemical testing and theoretical calculations that need further discussion and data supplement:

Reply: We sincerely appreciate the reviewer's thorough evaluation of our manuscript and the insightful, constructive feedback regarding the fundamental studies, electrochemical testing and theoretical calculations. We fully recognize the importance of addressing these issues and, in response, have undertaken comprehensive additional work, including experimental characterizations and theoretical calculations, to address these concerns-specifically the role of Cu valence in the hydrogenation reaction. We have made the necessary revisions to enhance the robustness and clarity of our findings. We remain committed to improving the quality of our work and ensuring that it meets the reviewer's expectations.

Comment 1. The same materials and the same reaction have been reported by Jiao (Nat. Commun. 2021, 12, 1949) and Wang (Nat. Commun. 2023, 14, 3847) successively. The FE in this work is ~95%, which is roughly the same as previously reported (~94.6%, Nat. Commun. 2021, 12, 1949). So, compared with the above-mentioned catalytic

system, I could not find the innovation and importance of this one and is only an addition to the field. What's more, the authors said, "... suggests a new strategy to enhance the electrochemical hydrogenation of organic molecules by regulating the Volume step". Questions like what happens to the other types of organic molecules by regulating the Volume step must be addressed.

Reply: Thank you very much for raising this question. Previous studies primarily focused on metallic Cu-based electrocatalysts, which were typically prepared by reducing Cu oxides through electrochemical treatment or thermal reduction (Nat. Commun. 2023, 14, 3847; Nat. Commun. 2023, 14, 3847). The reported stability of the metallic Cu-based electrocatalysts was less than 20 hours. In contrast, our manuscript introduces a CuO@Cu catalyst, prepared by electrochemical treatment of a Cu_2O film in the presence of acetonitrile. In this process, a disproportionation reaction occurs, converting Cu_2O into CuO and Cu, rather than fully reducing Cu_2O to metallic Cu. This CuO@Cu catalyst demonstrates exceptional stability and ethylamine selectivity (>95%) at a current density of 0.2 A cm^{-2} over 1000 hours. We further show that the hydrogen evolution reaction (HER) is effectively halted at the Volmer step, where protons migrate to the unsaturated bond of acetonitrile adsorbed on the CuO@Cu surface, thus facilitating the subsequent ARR process. The efficient migration of reductive protons to acetonitrile also contributes to the high stability of CuO@Cu under high current density. Considering these results, it suggests that metal oxides can maintain their oxide structures in the electrochemical hydrogenation of organic molecules (such as toluene, alkynes, or glycerol) by regulating the Volmer step. We have revised the related discussion in the manuscript.

In Page 1 of the revised manuscript: "This study suggests a new strategy to enhance the electrochemical hydrogenation of organic molecules by regulating Volmer step to prevent the reduction of oxide-based catalysts."

Comment 2. The study demonstrates that the material comprises oxidized copper, as

evidenced by a series of off-site characterizations. However, it should be noted that copper is highly susceptible to oxidation and phase transitions in an alkaline electrolyte environment. Consequently, off-site characterization could potentially result in misleading conclusions.

Reply: We sincerely appreciate the reviewer's insightful comment. We would like to emphasize that the presence of acetonitrile is crucial in preventing the reduction of Cu oxides. As shown in **Figure S2**, in the absence of acetonitrile, the Cu oxide undergoes reduction to metallic Cu under cyclic voltammetry (CV) conditions. In contrast, no reduction peak is observed when acetonitrile is present in the electrolyte. Moreover, the color of the CuO@Cu electrode before and after the 1000-hour test at 0.2 A cm^{-2} remains unchanged (black), which corresponds to the color of Cu oxide. However, when the CuO@Cu electrode is tested for HER without acetonitrile in the electrolyte under the same current density for 12 hours, the electrode surface turns reddish-orange (**Figure S13**), indicative of metallic Cu formation. In addition, we performed in-situ and operando X-ray absorption spectroscopy (XAS) to investigate the variation in Cu valence during electrochemical operation. First, Cu K-edge XAS spectra was recorded at open circuit potential (OCP), followed by Cu K-edge XAS spectra during CV cycling in the range of -0.8 V vs. RHE to -1.2 V vs. RHE. The sample was then subjected to chronoamperometric testing at -1.0 V vs. RHE for 1 hour, and Cu K-edge XAS spectra was collected again under the chronoamperometric testing. The energy position of the Cu K-edge was determined from the first maximum of the derivative spectrum. As shown in **Figure S14**, the Cu K-edge energy position did not shift during the electrochemical tests, indicating that the Cu valence remained stable. These results clearly demonstrate that the CuO@Cu catalyst maintains its oxide form during the acetamide reduction reaction (ARR), without undergoing reduction. The revisions are as follows:

In Page 3 of the revised manuscript: "We should emphasize that the presence of AN is crucial in suppressing the reduction of Cu oxides. As show in **Figure S2**, in the absence of AN, the Cu oxides are reduced to under the same electrochemical operation.

However, no reduction peak is observed when acetonitrile is present in the electrolyte."

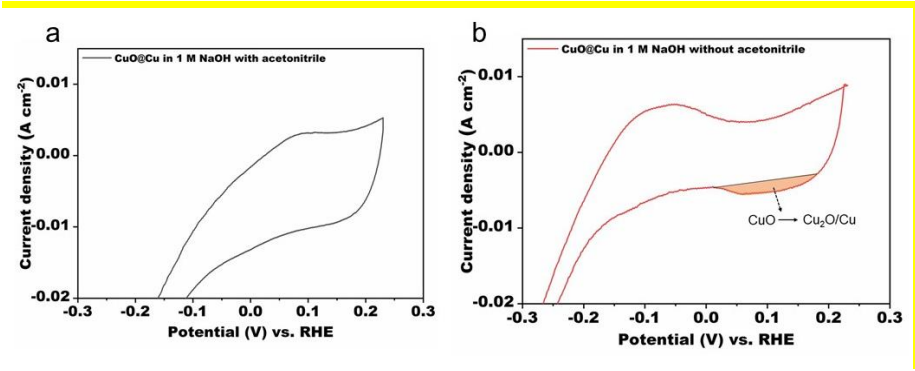

Figure S2. CV curves of CuO@Cu heterostructure in 1.0 M KOH with and without acetonitrile.

In Page 7 of the revised manuscript: "Furthermore, the color of the CuO@Cu electrode before and after the 1000-h test at 0.2 A cm^{-2} remains unchanged (black), which corresponds to the color of Cu oxide (**Figure S12**). In contrast, when the CuO@Cu electrode undergoes HER operations (without acetonitrile in the electrolyte) at the same current density for 12 hours, its surface turns reddish-orange, indicative of metallic Cu formation (**Figure S13**)."

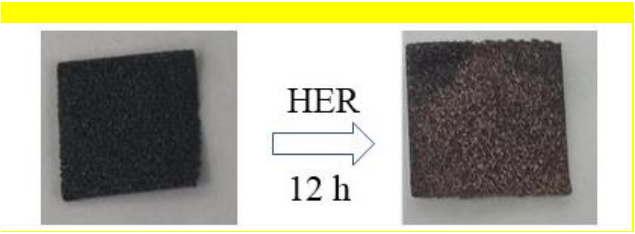

Figure S13. Photos of CuO@Cu electrode before and after HER operations at a current density of 200 mA cm^{-2} in 1 M NaOH without acetonitrile.

In Page 8 of the revised manuscript:

We also performed in-situ and operando X-ray absorption spectroscopy (XAS) under electrochemical operating conditions to further investigate the variation in Cu valence of the CuO@Cu catalysts. The Cu K-edge energy position was determined from the first peak in the derivative of the XAS spectrum. As shown in **Figure S15**, the energy

position of the Cu K-edge is not shifted during electrochemical operation, indicating that the Cu valence remained unchanged.

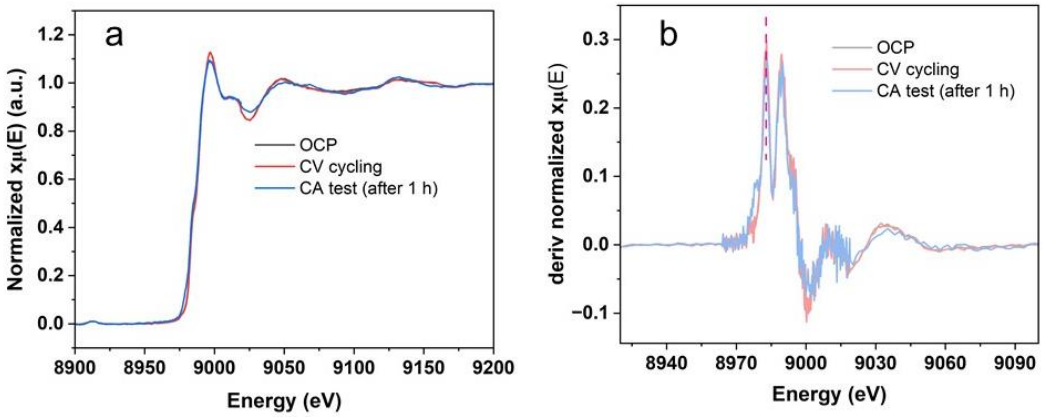

Figure S15. in situ Cu K-edge XANES spectra (a) and the corresponding first derivative (b).

In Page 4 of the revised Supplementary Materials: "The X-ray absorption spectra (XAS) measurements for the Cu K-edge were conducted in transmission mode (fluorescence mode) on the Laboratory-Based XAFS and XES Spectrometer (easyXAFS300+, USA). The energy was calibrated using corresponding metal foil as references. XANES and EXAFS data reduction and analysis were analyzed by Athena 3 and Artemis software. For the measurement, the CuO@Cu catalyst was carefully sonicated from the electrode and then collected. Cu XAS was firstly recorded at open circuit potential (OCP), followed by XAS during CV cycling in the range of -0.8 V vs. RHE to -1.2 V vs. RHE. The sample was then subjected to chronoamperometric testing at -1.0 V vs. RHE for 1 hour, and XAS was collected again under these conditions."

Comment 3. The reduction potential for the acetonitrile reduction reaction is found to be less than that required for the reduction of Cu^{2+} to metallic copper. This reaction process seems unreasonable and contradicts the test results given by Figure 1g that there is obviously a dissolution of Cu_2O and electrochemical redeposition process in the

electrochemical CV scanning. At such negative potentials or high current densities, can the Cu^{2+} in CuO@Cu stably exist? Or in fact, the real catalyst for the hydrogenation of nitriles is not the same as the CuO@Cu discussed in this work.

Reply: We agree that the reduction potential for acetonitrile reduction is lower than that required for the reduction of Cu^{2+} to metallic copper. However, as addressed in the reply to Comment 2, for CuO@Cu, HER was halted at the Volmer step, where the protons migrate to the unsaturated bond of AN adsorbed on CuO@Cu to facilitate the ARR reduction. The facile migration of the reductive protons to AN also explains the high stability of CuO@Cu under a high current density. **Figure 1g** describes the Cu leaching during the CV activation for the formation of CuO@Cu from Cu_2O. The Cu^{2+} leaching should be due to the reconstruction of Cu_2O, and be recaptured to form CuO, since no reductive peak is observed in the CV curve (**Figure S2**). More evidences for the high stability of CuO@Cu for ARR has been supported in the reply of Comment 2.

Comment 4. In an alkaline environment, the choice to utilize PEM instead of an anion exchange membrane (AEM) for flow cell experiments suggests a lack of profound insight into the fundamental principles of membrane electrode assembly devices on the part of the author.

Reply: We thank the reviewer for raising this question out. In our study, we tried to use an anion exchange membrane (FAA-PK-130) in the liquid flow cell. However, due to its poor stability in the presence of acetonitrile, the membrane was easily damaged, as shown in **Figure R1** below. As a result, we switched to using the more stable Nafion 117 membrane to separate the anode and cathode. We agree that the Nafion 117 membrane may increase the local acidity on its surface. However, since we did not assemble a membrane electrode system and the electrodes are self-supported, this configuration minimizes the impact of the membrane's local acidity. It is also worth noting that proton exchange membranes have been used in alkaline media in many studies [*Nat. Commun.*, 2021, 12, 1949; *Appl. Energy, 2019, 113323; J. Mater. Chem.*

A, 2022, 10, 13987-13997; J. Electroanal. Chem., 2022, 116680]. We have added the related discussion in the manuscript: "Nafion 211 was used for its relatively high stability in the presence of AN."

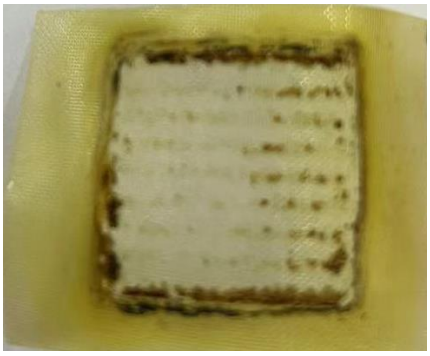

Figure R1. Photo of FAA-PK-130 after ARR test.

Comment 5. In the stability test depicted in Figure 2, the pronounced selective fluctuation observed for ethylamine within the initial 100 hours is intriguing. Could this be attributed to alterations in the material's structural integrity? For ^{1}H NMR tests, the author should provide internal standard curve of ethylamine. The author should describe the Faraday efficiency test method and producer in the stability test. In Figure S7, ^{1}H NMR spectrum of the liquid products after 1000 hours test, peaks area belongs to ethylamine are significantly smaller than that of other samples, but the Faraday efficiency given in the text is still higher than 95%.

Reply: We appreciate the reviewer's careful attention to the Faraday efficiency (FE) results. At the beginning of the chronoamperometry test, we measured the FE at small intervals, which may lead to the more noticeable fluctuations in the initial 100 hours. However, as show in **Figure R2,** the fluctuation in the initial 100 hours is not notably more significant than those of other stages after we plotted the FE average line in the **Figure R2**.

For the ^{1}H NMR measurement, TMS in deuterated methanol was used as the internal standard for FE calculation. The EA content was determined based on the ratio of the ethylamine peak area to the TMS peak area. It is important to note that during our

stability test, the electrolyte was refreshed every 12 hours, so the sample used for ^{1}H NMR analysis was not accumulated over time. In addition, the general signal intensity of H^{1} NMR is also related to the sample amount used in the H^{1} NMR measurement. In **Figure S11**, although peaks area belongs to ethylamine are smaller than that of other samples, the TMS signal is also smaller than that of other samples. The calculated FE based on the ratio of the peak area of ethylamine to the peak area of the internal standard of TMS is 96%. We have added additional experimental details in Supplementary Materials.

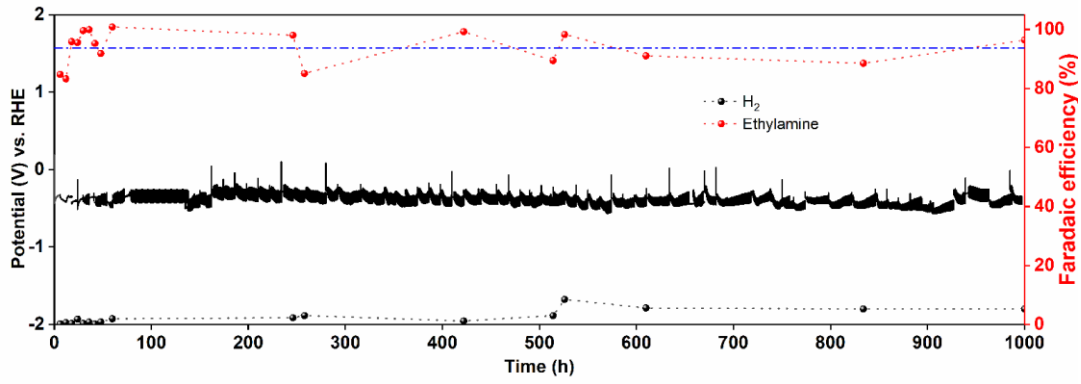

Figure R2. Faraday efficiencies during the chronoamperometry test.

In Page 3 of the revised Supplementary Materials:

1.4 Chronopotentiometry test

Chronopotentiometry experiments were performed in a H-type cell to evaluate the performance of acetonitrile electroreduction using a three electrode-system. The Ag/AgCl electrode was employed as the reference electrode, and a platinum net was used as the counter electrode. The electrolyte was refreshed every 12 hours. The measured potentials were corrected using iR compensation to account for the voltage drop caused by solution resistance. For each data point of Faraday efficiencies, 400 uL of liquid product was collected at intervals and the corresponding time was recorded.

1.5 Flow cell measurement

A two-compartment microfluidic flow cell electrolyzer was fabricated for ARR electrolysis. NiFe LDH (1 cm × 1 cm) and CuO@Cu (1 cm × 1 cm) were employed as the anode and cathode, respectively. A Nafion 117 membrane was used to separate the

anode and cathode. The catholyte consisted of 1 M NaOH with 12 wt% acetonitrile, while the anolyte was 1 M NaOH. The flow rate for both catholyte and anolyte was 10 mL min^{-1}.

Comment 6. The authors contend that a synergistic interaction between Cu and Cu^{2+} is pivotal in the electrochemical hydrogenation of acetonitrile. Consequently, they propose the preparation and subsequent electrochemical evaluation of a range of Cu and Cu^{2+} compositions with varying proportions to elucidate this synergistic effect.

Reply: Thanks for your comment. In our manuscript, CuO is identified as the active component while metallic component facilitates the electron transfer. We suggest a synergistic hydrogenation process that contributes to the ARR. This process involves both surface hydrogen migration and proton addition from the solution. Since the formation of CuO@Cu results from a disproportionation reaction of Cu_2O during CV cycling at negative potentials ($Cu_2O \rightarrow Cu + CuO$), the ideal ratio of Cu and Cu^{2+} composition should be close to 1:1 and cannot be tuned in this system. Nevertheless, the reviewer's suggestion has inspired new avenues for further investigation, which we intend to explore in our future work.

Comment 7. In-situ infrared spectroscopy conducted under open circuit potential (OCP) conditions may yield deceptive results, as Cu is subject to phase transformations over time within a highly alkaline environment. Consequently, the adsorption data obtained may not accurately reflect the properties of the initial material. Furthermore, the authors have not thoroughly annotated the infrared absorption peaks, such as those at 1340 and 1180 cm^{-1}, among others. In addition, the adsorption modes, such as adsorption via only the N atom or both the C and N atoms, of various molecules should be optimized and illustrated because different adsorption models lead to different shifts in FTIR. The simulated results should be compared with the experiment data to exactly determine the adsorption of the reaction species, hence a more accurate reaction mechanism.

Reply: Thanks for the valuable comments. In our manuscript, the in situ attenuated total internal reflectance Fourier transform infrared spectroscopy (ATR-FTIR) was not measured under OCP condition, but under the electrochemical ARR operations. In the in situ ATR-FTIR measurement, we established the system spectrum under open circuit conditions as a baseline, monitoring spectral changes under electrochemical operations -0.146 V vs. RHE over time. To make it clear, we provide the illustration of the ATR-FTIR setup (**Figure S18**). The adsorption mode was employed for the FTIR signal collection, which means the positive peaks are the signals of the generated species. The peak at 1340 cm^{-1} is a negative peak, and this peak is also present in OCP baseline, which suggests that this peak is a noise. The tiny peak at 1180 cm^{-1} is also a negative one, which can be considered as the downhill for the positive peak at 1133 cm^{-1}. We have added the ATR-FTIR experiment details.

In Page 4 of the revised Supplementary Materials: "In-situ SEATR-FTIR measurements were performed using a Linglu Instruments ECIR-II cell mounted on a Nicolet-6700 Fourier transform infrared spectrometer. The cell featured a single-bounce silicon crystal coated with an Au membrane (**Figure S18**), operated in internal reflection mode. Chronoamperometry (CA) experiments were monitored using a CHI 760E electrochemical workstation. The in-situ electrochemical FT-IR cell was configured as a three-electrode system, with an Ag/AgCl electrode as the reference, a Pt wire as the counter electrode, and the CuO@Cu catalyst as the working electrode. The CuO@Cu catalyst was carefully sonicated from the electrode and loaded on the Au membrane as working electrode. The electrolyte consisted of 1 M NaOH with 12 wt% acetonitrile. The spectra were firstly recorded at OCP, and this point was set as 0 s. Then the potential was held -0.146 V vs. RHE and maintained 3000 s by CA method. The in-situ FTIR was recorded at 10, 100, 200, 300, 500, 800, 1000, 1500, 2000, 3000 s during CA method."

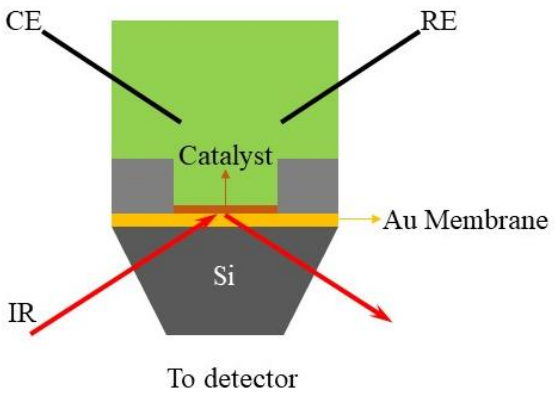

Figure S18. The schematic diagram of in situ attenuated total internal reflectance Fourier transform infrared device. RE: reference electrode; CE: counter electrode.

In addition, we simulated the vibrational spectra of various species adsorbed on the CuO_x surface, as shown in Table S3 in Supplementary Materials. The peaks between 1100 and 1300 cm^{-1} are mainly annotated as the modes of C-N bond stretching. As the hydrogenation proceeds, the C-N bond is weakened and the absorption peak is generally red-shifted. Especially, the peaks at 2273 and 1133 cm^{-1} in the spectrum were supposed to correspond to the reactant and product, respectively, in agreement with the simulated vibrational frequencies. In previous manuscript, we attributed the peaks at 1133, 1241, 1297 cm^{-1} to N-H_x. We now have revised the "N-H_x" to "C-NH_x" in the manuscript.

In Page 10 of the revised manuscript: "In **Figure 4g**, the peaks at 1133, 1241, 1297 cm^{-1} suggests the presence of C-NH_x, according to previous study and our theoretical calculation (**Table S3**). As the hydrogenation proceeds, the C-N bond is weakened and the absorption peak is generally red-shifted. We attribute the 1241 cm^{-1} and 1297 cm^{-1} to the C-N bond stretching of the initial hydrogenated specie."

In Page 34 of the revised Supplementary Materials:

Table S3. Simulated vibrational modes and corresponding frequencies of various intermediates. Vibrational frequencies close to experimental ATR-FTIR results were listed. Considering the experimental frequency of C≡N stretching is 2273 cm^{-1}, a scaling factor as 0.9887 is employed to corrected the simulated frequencies, which are labeled in the brackets.

Adsorption structures	Vibrational frequency / cm^{-1}	Vibrational mode	Experimental frequency / cm^{-1}
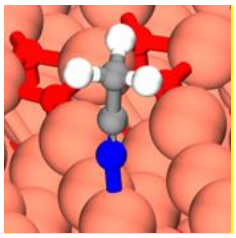	2299 (2273)	C≡N stretching	2273
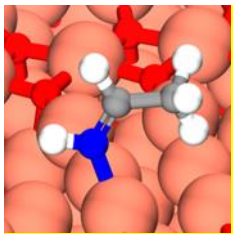	1283 (1269)	CH=NH stretching	1297
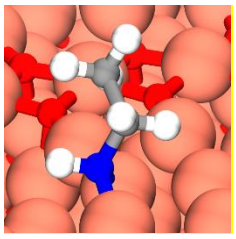	1297 (1282)	CH_2-NH stretching	
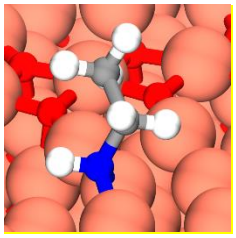	1234 (1220)	CH_3-CH_2-NH twisting	1241
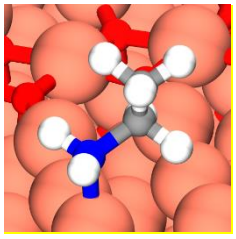	1149 (1136)	CH_2-NH_2 stretching	1133

Comment 8. On what basis is the model for the DFT calculations constructed? Analyzing the results reveals a discrepancy where the material contains a significantly higher proportion of Cu than Cu^{2+}, yet the model inversely represents a greater abundance of Cu^{2+} over Cu. Models that are incongruent with experimental findings

may yield deceptive outcomes. The vacuum layer in the Z direction is set to 12 Å, but considering that the authors placed more than 6 water molecules clusters as proton donors, a vacuum layer thickness greater than 15 Å is recommended.

Reply: The simulated CuO_x model is constructed based on the structural characterization of XRD spectrum after ARR stability test, which indicates that the frame of CuO is maintained in CuO@Cu. TEM images of CuO@Cu shows obvious CuO (002) crystal plane as well. According to Auger spectroscopy results, the signal for Cu^0 was enhanced after ARR, whereas Cu^{2+} signal still dominates in the surface of CuO@Cu. To simulate the partially reduced surface, the theoretical model named as CuO_x was constructed based on CuO (001) slab, in which all the surface oxygen atoms and half of the subsurface oxygen atoms were removed. Herein, there exists Cu^0-rich environment as you suggested, while CuO matrix is maintained. The optimized CuO_x slab model demonstrates both Cu^0-rich region containing Cu-Cu coordination structures and Cu^{2+}-rich region containing $Cu\text{-}O_4$ coordination structures similar to that in CuO matrix. Bader charge analysis further confirms the coexistence of Cu^0 and Cu^{2+} with ratio close to 1:1 in the surface. The partially reduced $Cu^{\delta+}$ ($0 < \delta < +1$) species are located between Cu^0 and Cu^{2+} region. In general, we suspect that our CuO_x model retains the main features of CuO@Cu characterized in experiment, and thus could reflect its properties in some extent. We understand that more metallic Cu was characterized in the XRD text mainly due to the metallic Cu as the substrate, but limited by the size of the model that the DFT calculation can handle, such a slab model that includes Cu^0 in the surface and maintains the CuO matrix is relatively reasonable. Descriptions of the simulated CuO_x model was adjusted for better understanding of our CuO_x model.

In Page 5 of the revised Supplementary Materials: "Based on the experimental XRD, TEM and Auger spectroscopy characterizations, a partially reduced CuO_x slab model was constructed to represent the CuO@Cu catalyst. A 4×4 CuO (001) supercell was used, in which all the surface oxygen atoms and half of the subsurface oxygen atoms were removed. The optimized CuO_x slab (**Figure S20**) maintains CuO (001) matrix,

while there exhibits Cu^0 and Cu^{2+} with ratio close to 1:1 in the surface, validated by the Bader charge analysis shown in **Figure S21**."

We further carried out DFT calculations by setting thickness of the vacuum layer as 15 and 17 Å, to compare with the results using a vacuum layer of 12 Å in the manuscript. The results in **Table R1** show that the energy differences are within 0.05 eV, which would not alter the conclusions regarding the hydrogenation mechanism and the activity comparison between Cu (111) and CuO_x in this work. Indeed, the results using the thicker vacuum layer should be more accurate. We will carefully test the thickness of the vacuum layer and utilize the thicker vacuum layer in our future studies. Thanks again for your kind suggestion.

Table R1. DFT energies calculated with different thicknesses of vacuum layer. The energy differences are within 0.05 eV between thicknesses set as 12, 15 and 17 Å.

Thickness of vacuum layer	*CH_3CN / eV	TS #CH_3C-HN / eV	*CH_3CHN / eV
12 Å	-411.983	-410.929	-411.111
15 Å	-411.963	-410.929	-411.117
17 Å	-411.957	-410.929	-411.119
Atomic structures	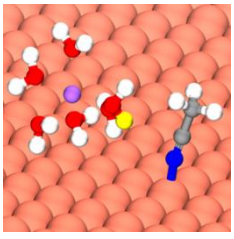	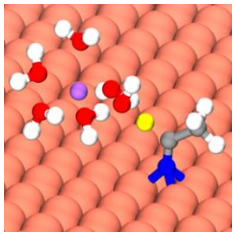	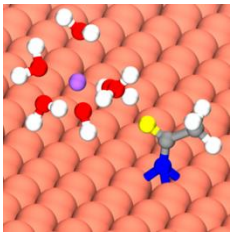

Comment 9. In the DFT calculations, the authors postulate that the reduction of acetonitrile proceeds firstly via the Volmer step, involving the decomposition of H_2O. The reader is left to ponder why the protons from water do not directly attach to the acetonitrile molecules, but instead are first dissociated onto the material's surface before being transferred to the acetonitrile for hydrogenation? During the

hydrogenation of acetonitrile to ethylamine, the asymmetry of the acetonitrile molecule suggests the existence of multiple potential reaction pathways. The authors should meticulously evaluate these paths to identify the most favorable reaction trajectory.

Reply: We sincerely thank the reviewer for these helpful suggestions to improve our manuscript. The Bode and DRT experiments indicated that the surface adsorbed hydrogen (*H) is involved in the hydrogenation of acetonitrile. Whether or not the acetonitrile is hydrogenated, Volmer step takes place under the applied potential, leading to the generation of the adsorbed hydrogen (*H). In our work, all possible intermediates and reaction pathways were firstly simulated according to computational hydrogen electrode (CHE) model, as shown in **Figure S22**. The thermodynamically favorable reaction pathways on CuO_x and metallic Cu surfaces were screened out for further discussion. Subsequently, the kinetic barriers on these two thermodynamically favorable paths were calculated to examine whether the hydrogen atom in each hydrogenation step is from *H or proton in H_2O, as shown in **Figure S23** and **S24**. Under −0.4 V (vs. RHE), hydrogenation towards C site via *H migration is kinetically preferred to that via proton transfer from H_2O. On the contrast, protons in water, rather than *H, binds more readily to N site. It is understandable that the C site is positive charged and prefers *H on the metal surface with negative charge, whereas the negatively charged N site is attractive to the positively charged proton in H_2O (**Table S4**). It should be noted that this situation is not unique in ARR, but also similar to the electrochemical reduction of CO_2. It has been reported that the hydrogenation of C site favors the *H mechanism, while that of O site prefers the proton from aqueous H_2O (*Angew. Chem. Int. Ed.* 2013, 52 (9), 2459-2462.; *J. Am. Chem. Soc.* 2017, 139 (1), 130-136.). We have added relevant discussion in the revision.

In Page 12 of the revised manuscript: "All possible intermediates and reaction pathways were firstly simulated according to computational hydrogen electrode (CHE) model, as shown in **Figure S22**. The thermodynamically favorable pathways on CuO_x and metallic Cu surfaces were screened out. Considering an external potential of −0.4

V (vs. RHE), the kinetic barriers on these two thermodynamically favorable paths were calculated to examine whether the hydrogen atom in each hydrogenation step is from *H or proton in H_2O, as shown in **Figure S23-24**."

In Page 13 of the revised manuscript: "It is understandable that the positively charged C atoms may prefer the surface *H with partially negative charge, while the negatively charged N atom is attractive to the positively charged proton in H_2O (**Table S4**). Similar situation has been reported in electrochemical reduction of CO_2, where the hydrogenation of C atoms favors the surface hydrogen, while the hydrogenation of O atoms prefers the proton from aqueous H_2O [26, 27]."

In Page 28~30 of the revised Supplementary Materials:

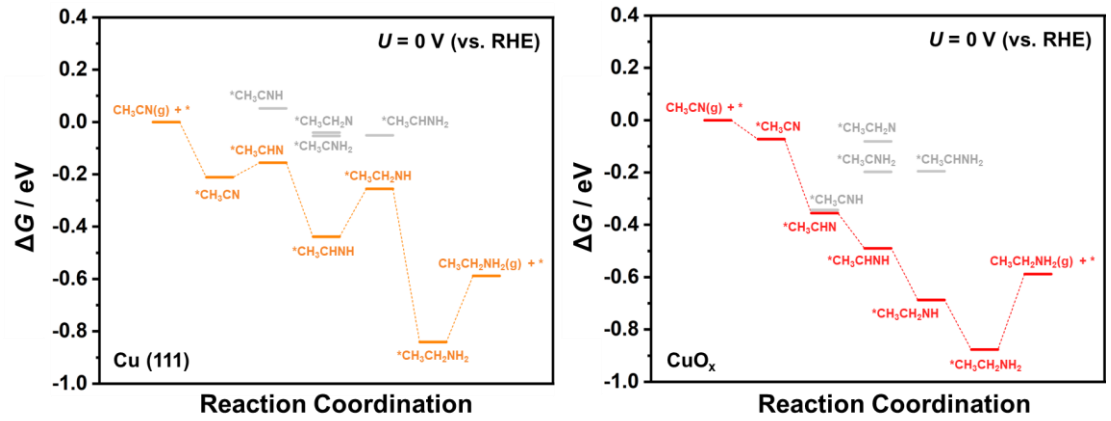

Figure S22. Free energy diagrams for acetonitrile electroreduction over Cu (111) (left) and CuO_x (right) at an external potential $U = 0$ V (vs. RHE).

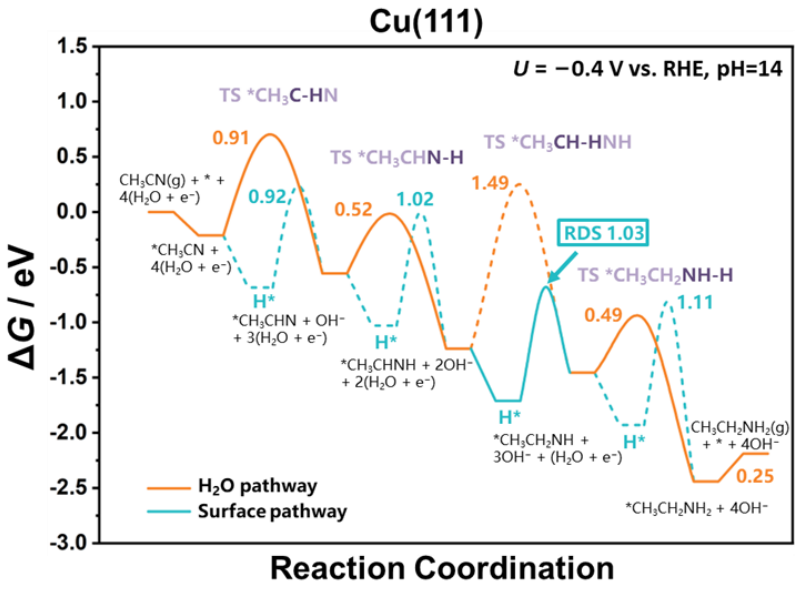

371

372 **Figure S23.** Free energy diagrams for acetonitrile electroreduction along H_2O pathway
373 (orange line) and surface pathway (blue line) over Cu (111) at an external potential U
374 = −0.4 V (vs. RHE, pH = 14). Pathway with lower barrier is shown in solid line.

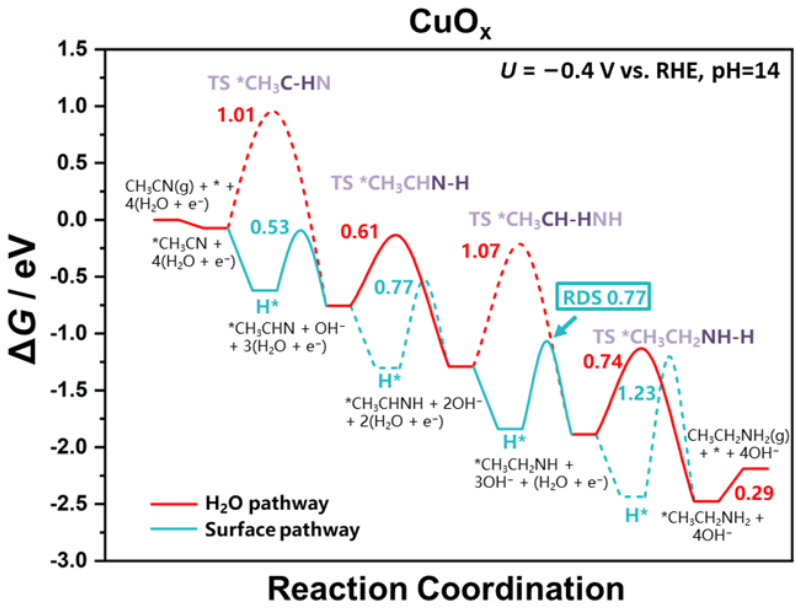

375

376 **Figure S24.** Free energy diagrams for acetonitrile electroreduction along H_2O pathway
377 (red line) and surface pathway (blue line) over CuO_x at an external potential U = −0.4
378 V (vs. RHE, pH = 14). Pathway with lower barrier is shown in solid line.

379

In Page 35 of the revised Supplementary Information:

Table S4. Bader charge (|*e*|) of hydrogen in *H, aqueous H_2O, and C, N atoms in cyano group of adsorbed acetonitrile.

	Cu (111) / |*e*|	CuO_x / |*e*|
*H	−0.28	−0.23
H in H_2O	0.69	
C in -CN of *CH_3CN	0.82	0.80
N in -CN of *CH_3CN	−1.21	−1.17

Reviewer #2 (Remarks to the Author):

Tang et al. presented a CuO@Cu heterostructure catalyst with remarkable stability in the electroreduction of acetonitrile to ethylamine with negligible degradation over a 1000-hour test at a current density of 0.2 A·cm^{-2}. Detailed investigation on the catalytic mechanism have been performed and a synergistic hydrogenation process is proposed based on both experimental and theoretical evidence. Before acceptance, necessary revision is required.

Reply: We are much appreciated for the reviewer's comments and suggestions to make a revision of our manuscript. The explanations, discussions and as well as additional experiments and theoretical calculations have been supplemented to the revised version of manuscript.

Comment 1. The LSV curve of CuO@Cu heterostructure in 1 M NaOH solution should be given to demonstrate that the reduction of acetonitrile to ethylamine occurs more readily than hydrogen evolution.

Reply: We have provided the LSV curve of CuO@Cu heterostructure in 1 M NaOH solution, and added the related discussion in the manuscript. The revision is as follows.

In Page 5 of the revised manuscript: "As shown in **Figure S4**, the reduction of acetonitrile to ethylamine occurs much more readily than hydrogen evolution."

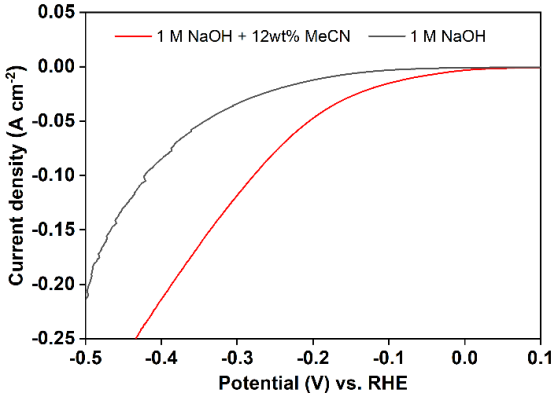

Figure S4. LSV curves of CuO@Cu heterostructure in 1 M NaOH solution with and without acetonitrile.

Comment 2. The most important key point of this study was the improvement of stability. Do authors have any explanation on the remarkable stability?

Reply: We appreciate the reviewer for raising this question regarding the explanation for the enhanced stability. For CuO@Cu, the hydrogen evolution reaction (HER) is halted at the Volmer step, where protons migrate to the unsaturated bond of acetonitrile (AN) adsorbed on the CuO@Cu surface. The rapid consumption of the reductive protons can significantly contribute to the high stability of CuO@Cu under high current density. We have added the related discussion in the revised manuscript. The revision is as follows:

In Page 9 of the revised manuscript: "The rapid consumption of the reductive protons can significantly contribute to the high stability of CuO@Cu under high current density."

Comment 3. A flow cell was assembled for the ARR test. I note that there is an activity enhancement after refreshing the electrolyte. Why?

Reply: Many thanks for the comment. As the ARR reaction progresses, the concentration of acetonitrile in the electrolyte decreases, while the concentration of ethylamine increases. This shift makes the adsorption of acetonitrile and the desorption of ethylamine more difficult over time. Therefore, when the electrolyte is refreshed, an increase in activity is observed.

Comment 4. The lattice fringes in HRTEM image (Figure 1e) are somehow unclear, please provide a clearer one, for example as an inset.

Reply: We sincerely thank the reviewer for this careful reading and helpful suggestion. We have provided a clearer HRTEM image.

Comment 5. Water cluster was considered in the calculation of the barrier for hydrogen

migration from solvent. Do the surrounding water molecules have any effect on the barriers for hydrogenation via surface adsorbed hydrogen?

Reply: In this work, the implicit solvation model was included throughout calculations, for both H_2O-involving and *H-involving pathways, to partially account for the solvation effect. The explicit water clusters were considered for H_2O-involving pathway since water molecules perform as the proton donor. While for the *H-involving pathway, the surrounding water cluster is supposed to have little effect as it does not participate in the hydrogenation process. Besides, several reports have shown that the local H_2O network could not promote the surface hydrogenation process of C atoms in electrocatalytic CO_2RR (*Angew. Chem. Int. Ed.* **2013**, 52 (9), 2459-2462.; *J. Am. Chem. Soc.* **2017**, 139 (1), 130-136.) In this work, the *H-involving hydrogenation without considering surrounding water molecules holds energetic priority over hydrogenation with aqueous H_2O. Disregarding the surrounding water molecules for *H hydrogenation step would not change the conclusion.

The relevant demonstration has been added in Page 6 of the revised Supplementary Materials:

For the barrier calculation, H_2O was chosen as the proton donor according to the alkaline conditions. Considering that OH^- ions need at least 3~4 H_2O molecules for solvation, an explicit hydrogen-bonded water cluster comprising 6 H_2O molecules was considered during searching for the transition state for aqueous H_2O pathway. A sodium atom was added to help simulating the reductive potential. All the water molecules were relaxed during transition state search. While for the surface adsorbed hydrogen pathway, the explicit water cluster was not included as the H_2O does not participate in the reaction process and should have little effect on the barrier. Barriers from various water cluster structures were investigated, and the lowest of which should dominate the activity. The charge extrapolation method [20-21] developed by Karen Chan et al. was applied to deduce the potential-dependent activation barriers. Combination of CHE model and the

charge extrapolation method has garnered validation as an effective tool for calculating free energy diagrams of electrocatalytic process, like HER [22] and CO_2RR [23]. When it involves hydrogenation via surface pathway, we assume that the barrier is independent with the electrode potential, premised on that there is no excess electron transfer during this process from the perspective of the charge extrapolation method.

Comment 6. Are the energies of the explicit water molecules included in the free energy profile? Are the energy changes derived from CHE model comparable to that calculated in the kinetic calculation?

Reply: We sincerely thank the reviewer for these helpful suggestions to improve our manuscript. The surrounding water molecules besides adsorbates were all relaxed during searching for transition states. The barriers include reconstruction energy of water clusters. Computational hydrogen electrode (CHE) model is the most prevalent method in examining the thermodynamics of electrocatalytic process. The barriers under targeted electrode potential were deduced with the charge extrapolation developed by Karen Chan et al. The reliability and efficiency of combination of the CHE model and the charge extrapolation method have been verified in exploring the free energy diagram of electrocatalytic process, including HER (*J. Phys. Chem. C* 2020, 124, 28083-28092) and CO_2RR (*Nat. Commun*. 2019, 10, 32). Corresponding description has been recomposed in Supplementary Information, as shown in the reply to Comment 5.

Comment 7. There are some typos in the manuscript, e.g., “Volume” in the Page 1 should be “Volmer”. The quality of the figures could also be improved.

Reply: Many thanks for the reviewer’s careful reading. We have revised the typos.

Reviewer #3 (Remarks to the Author):

The author constructed CuO@Cu Heterostructures were used to stabilize the electrocatalytic reduction of acetonitrile to ethylamine, showing good stability and Faraday efficiency. CuO was used as the active site, Cu enhanced electron transfer, and H* generated by Volmer step was transferred to the nearby acetonitrile to promote the reaction, which was verified by DFT. While the topic is of interest, there are several concerns and limitations that prevent the paper from being qualified for publication in Nature communications.

Reply: We sincerely appreciate the reviewer for their time and effort in providing valuable feedback that has greatly contributed to the improvement of our work. In response to the reviewer's comments, we have thoroughly addressed all concerns regarding the evidence and theoretical calculations. Additionally, we have conducted further experiments and included supplementary theoretical analyses to strengthen our claims and provide a more robust foundation for our conclusions.

Comment 1. The author said that the formation of CuO and Cu heterostructure, but did not demonstrate in this paper.

Reply: We sincerely thank the reviewer for raising this question. There are several evidences supporting the formation of a CuO and Cu heterostructure. Initially, we observed that Cu foam, oxidized with a Cu_2O surface layer, undergoes reconstruction during electrochemical cyclic voltammetry (CV) cycling at negative potentials. The resulting material exhibits a characteristic CuO structure on its surface, as shown by the black line in **Figure 1b**. Typically, Cu_2O cannot be oxidized at negative potentials, suggesting the occurrence of a disproportionation reaction: $Cu_2O \rightarrow Cu + CuO$. We further employed Cu $L_3M_{45}M_{45}$ Auger spectroscopy to probe this transformation. In the annealed Cu foam, Cu^+ predominates, consistent with the formation of Cu_2O. However, after CV activation in the presence of acetonitrile, the Cu^{2+} peak becomes dominant, and a Cu^0 peak emerges as a shoulder to the Cu^{2+} peak (**Figure 1c**), indicating the

formation of a CuO@Cu heterostructure. In addition, TEM images further confirm the coexistence of CuO and amorphous Cu domains (**Figure S15**), in agreement with the Auger spectroscopy results. Moreover, Raman analysis was also carried out to investigate the surface species. The peaks at 147 cm^{-1}, 217 cm^{-1}, and 632 cm^{-1} in the spectrum of the annealed Cu foam correspond to Cu_2O (**Figure 1d**). In comparison, the CuO@Cu heterostructure exhibits distinct characteristic peaks of CuO (98 cm^{-1}, 344 cm^{-1}, and 630 cm^{-1}). The absence of specific Cu_2O peaks in the spectrum of CuO@Cu heterostructure confirms the transformation of Cu_2O. Since metallic Cu do not show Raman signals, Cu substrate cannot be detected in the Raman spectra. These results clearly demonstrate the formation of CuO and Cu heterostructure.

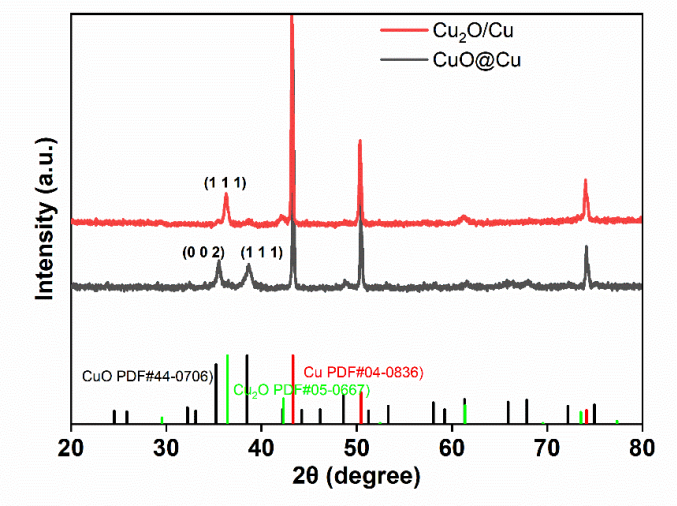

Figure 1b. XRD patterns of Cu_2O/Cu and CuO@Cu.

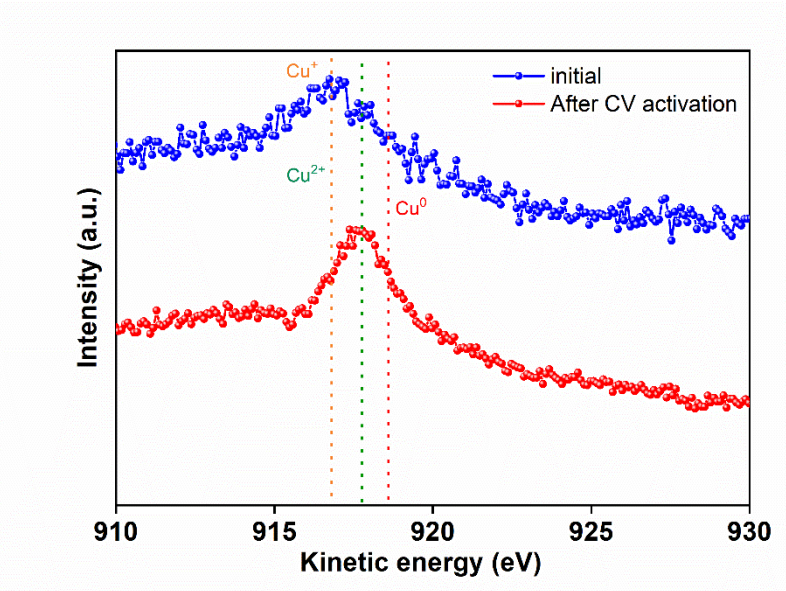

Figure 1c. L3M45M45 Auger spectra of Cu_2O/Cu and CuO@Cu; (d) Raman spectra of Cu_2O/Cu and CuO@Cu;

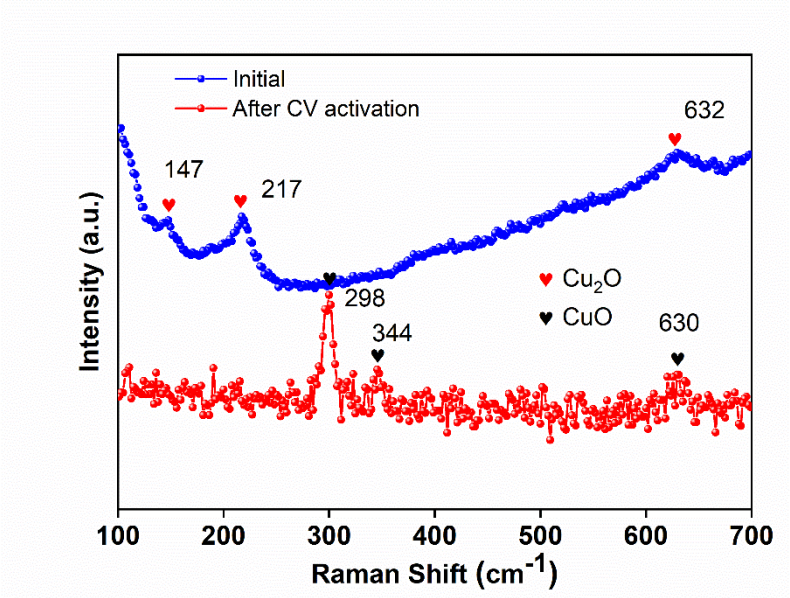

Figure 1d. Raman spectra of Cu_2O/Cu and CuO@Cu

Comment 2. The "Cu2 1O" in Figure 2b should be further defined as "Cu2+1O". What is the valence state of Cu in Cu2+1O? The red line is only described as Cu2O@Cu?

Reply: Many thanks for raising this question. Cu2 1O is the name in the JCPDS PDF database, which refers to Cu_2O. For clarity, we have updated it to Cu_2O. The valence of Cu in Cu_2O is +1. Since the Cu_2O@Cu is prepared through surface calcination of copper foam; therefore, we have revised this notation to Cu_2O/Cu to better reflect this.

Comment 3. Acetonitrile can be reduced to 3-aminobutyronitrile, ethane (C_2H_6), NH_3 and amines. What is the selectivity of producing ethylamine in this paper, and whether to produce other amine compounds.

Reply: Thanks for the comment. In our study, no 3-aminobutyronitrile, diethylamine, triethylamine or other amines were probed by H^1 NMR, nor did C_2H_6 is detected by gas chromatography, suggesting that the production of these compounds is negligible. Additionally, the Faradaic efficiency for EA was found to be over 95%, as determined

both from H^1 NMR and gas chromatography.

Comment 4. The CuO shell on the catalyst surface, according to Fig. 3C, after 1000h of catalysis, the Cu^0 valence peak is more obvious, while the Cu^{2+} peak intensity decreases. Whether there is reconstruction during the reduction process (CuO→Cu).

Reply: In our study, CuO@Cu was formed by a disproportionation reaction of Cu_2O ($Cu_2O \rightarrow Cu + CuO$). The theoretical mole ratio of Cu^{2+} to Cu should be 1:1. In **Figure 3c**, we can obverse that, after 1000-hour of catalysis, the Cu^+ is negligible and Cu^0 valence peak became more pronounced, suggesting a more complete transformation of Cu_2O to CuO@Cu. The peak intensities of Cu^0 and Cu^{2+} after the 1000 h test are much closer to each other, consistent with the theoretical mole ratio of 1:1.

In addition, we would like to emphasize that the presence of acetonitrile is crucial in preventing the reduction of Cu oxides. As shown in **Figure S2**, in the absence of acetonitrile, the Cu oxides undergo reduction to metallic Cu under cyclic voltammetry (CV) conditions. In contrast, no reduction peak is observed when acetonitrile is present in the electrolyte. Moreover, the color of the CuO@Cu electrode before and after the 1000-hour test at 0.2 A cm^{-2} remains unchanged (black), which corresponds to the color of Cu oxide. However, when the CuO@Cu electrode is tested for hydrogen evolution reaction (HER) without acetonitrile in the electrolyte under the same current density for 12 hours, the electrode surface turns reddish-orange (**Figure S13**), indicative of metallic Cu formation. In addition, we performed in-situ and operando X-ray absorption spectroscopy (XAS) to investigate the variation in Cu valence during electrochemical operation. First, Cu K-edge XAS spectra was recorded at open circuit potential (OCP), followed by Cu K-edge XAS spectra during CV cycling in the range of -0.8 V vs. RHE to -1.2 V vs. RHE. The sample was then subjected to chronoamperometric testing at -1.0 V vs. RHE for 1 hour, and Cu K-edge XAS spectra was collected again under the chronoamperometric testing. The energy position of the Cu K-edge was determined from the first maximum of the derivative spectrum. As shown in **Figure S14**, the Cu K-edge energy position did not shift during the electrochemical tests, indicating that the

Cu valence remained stable. These results clearly demonstrate that the CuO@Cu catalyst maintains its oxide form during the acetamide reduction reaction (ARR), without undergoing reduction. We have added related discussion in the manuscript. The revision is as follows:

In Page 3 of the revised manuscript: "We should emphasize that the presence of AN is crucial in suppressing the reduction of Cu oxides. As show in **Figure S2**, in the absence of AN, the Cu oxides are reduced to metallic C under the same electrochemical operation. However, no reduction peak is observed when acetonitrile is present in the electrolyte."

In Page 7 and 8 of the revised manuscript: "Furthermore, the color of the CuO@Cu electrode before and after the 1000-h test at 0.2 A cm^{-2} remains unchanged (black), which corresponds to the color of Cu oxide (**Figure S12**). In contrast, when the CuO@Cu electrode undergoes HER operations (without acetonitrile in the electrolyte) at the same current density for 12 hours, its surface turns reddish-orange, indicative of metallic Cu formation (**Figure S13**)……**In Figure 3c**, we can obverse that after 1000-h chronoamperometry measurement, the Cu^{+} is negligible and Cu^{0} valence peak became more obvious, suggesting a more complete transformation of Cu_2O to CuO@Cu. The peak intensities of Cu^{0} and Cu^{2+} after the 1000-h test are much closer to each other, consistent with the theoretical mole ratio of 1:1. We performed in-situ and operando X-ray absorption spectroscopy (XAS) under electrochemical operating conditions to further investigate the variation in Cu valence of the CuO@Cu catalysts. The Cu K-edge energy position was determined from the first peak in the derivative of the XAS spectrum. As shown in **Figure S14**, the energy position of the Cu K-edge is not shifted during electrochemical operation, indicating that the Cu valence remained unchanged."

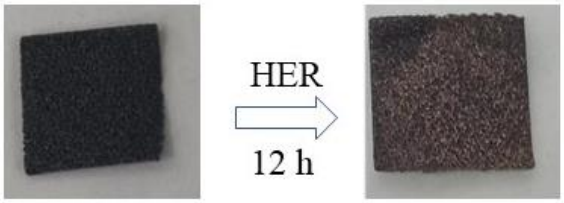

Figure S13. Photos of CuO@Cu electrode before and after HER operations at a current density of 200 mA cm^{-2} in a 1 M NaOH without acetonitrile.

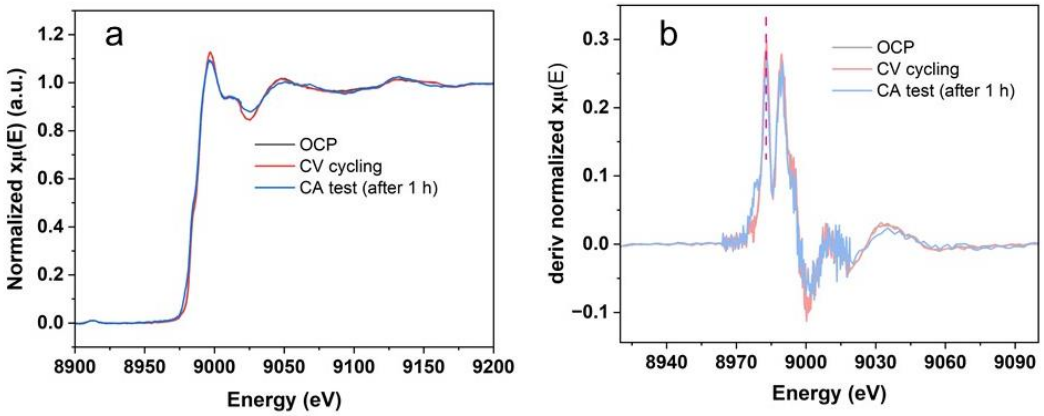

Figure S15. Cu K-edge XANES spectra (a) and the corresponding first derivative (b).

In Page 4 and 5 of the revised Supplementary Materials: "The X-ray absorption spectra (XAS) measurements for the Cu K-edge were conducted in transmission mode (fluorescence mode) on the Laboratory-Based XAFS and XES Spectrometer (easyXAFS300+, USA). The energy was calibrated using corresponding metal foil as references. XANES and EXAFS data reduction and analysis were analyzed by Athena 3 and Artemis software. For the measurement, the CuO@Cu catalyst was carefully sonicated from the electrode and then collected. Cu XAS was firstly recorded at open circuit potential (OCP), followed by XAS during CV cycling in the range of -0.8 V vs. RHE to -1.2 V vs. RHE. The sample was then subjected to chronoamperometric testing at -1.0 V vs. RHE for 1 hour, and XAS was collected again under these conditions."

Comment 5. The orange solid line in Figure 5b represents CuO_x, but the specific valence state of Cu is not clear. As a comparison of the reaction path (CuO), the best reaction site and path should be given.

Reply: According to the Bader Charge analysis in **Figure S21**, there are Cu^0, $Cu^{\delta+}$ ($0 < \delta < 1$) and Cu^{2+} species in CuO_x slab model. From the DFT optimized structures of intermediates and transition states (**Figure 5c, Figure S26**), the reaction site of CuO_x are the reduced species, including Cu^0 and $Cu^{\delta+}$ ($0 < \delta < 1$). All the potential ARR paths have been examined and shown in **Figure S22**. The reaction pathway considered in the manuscript is the thermodynamically favored path, in which the hydrogenation process undergoes through $*CH_3CHN$, $*CH_3CHNH$, $*CH_3CH_2NH$ and $*CH_3CH_2NH_2$ intermediates, sequentially. Since CuO can be reduced under the negative potential, also confirmed by experimental characterization, the ARR pathway on CuO_x slab model is compared with that on metallic Cu, rather than CuO. We have recomposed the expression to make the description on reaction site and path clearer.

In Page 12 of the revised manuscript:

"All possible intermediates and reaction pathways were firstly simulated according to computational hydrogen electrode (CHE) model, as shown in **Figure S22**. The thermodynamically favorable pathways on CuO_x and metallic Cu surfaces were screened out. Considering an external potential of −0.4 V (vs. RHE), the kinetic barriers on these two thermodynamically favorable paths were calculated to examine whether the hydrogen atom in each hydrogenation step is from *H or proton in H_2O, as shown in **Figure S23-24**. …….. On CuO_x surface, ARR takes place on Cu^0 and $Cu^{\delta+}$ ($0 < \delta < 1$) (**Figure 5c, Figure S21, Figure S26**). Though the CH_3CN adsorption is slightly weakened, the activation towards $*CH_3CHN$ is significantly promoted with a barrier of 0.53 eV, in which surface hydrogen addition is dominant."

In Page 27 of the revised Supplementary Information:

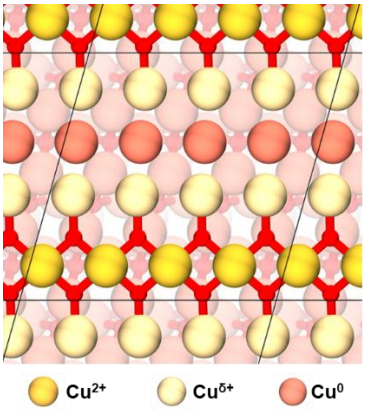

Species	Cu	Cu_2O	CuO	CuO_x surface		
Structure	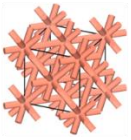	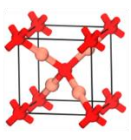	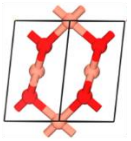			
Bader charge / |e|	0	+0.53	+0.97	+0.03	+0.24	+1.01

Figure S21. Bader charge analysis of Cu in CuO_x surface, Cu, Cu_2O and CuO. The results show that the CuO_x surface comprises Cu^0, Cu^{2+} and $Cu^{\delta+}$.

In Page 28 of the revised Supplementary Information:

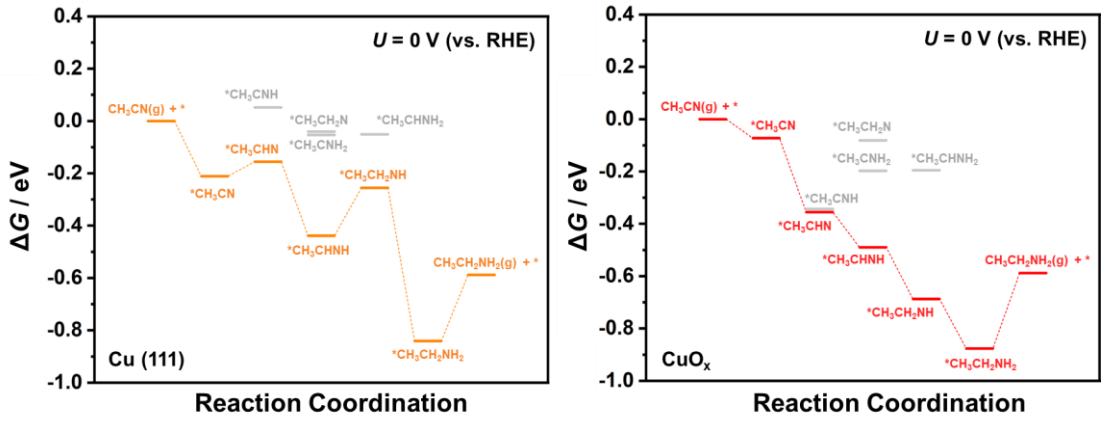

Figure S22. Free energy diagrams for acetonitrile electroreduction over Cu (111) (left) and CuO_x (right) at an external potential $U = 0$ V (vs. RHE).

In Page 32 of the revised Supplementary Information:

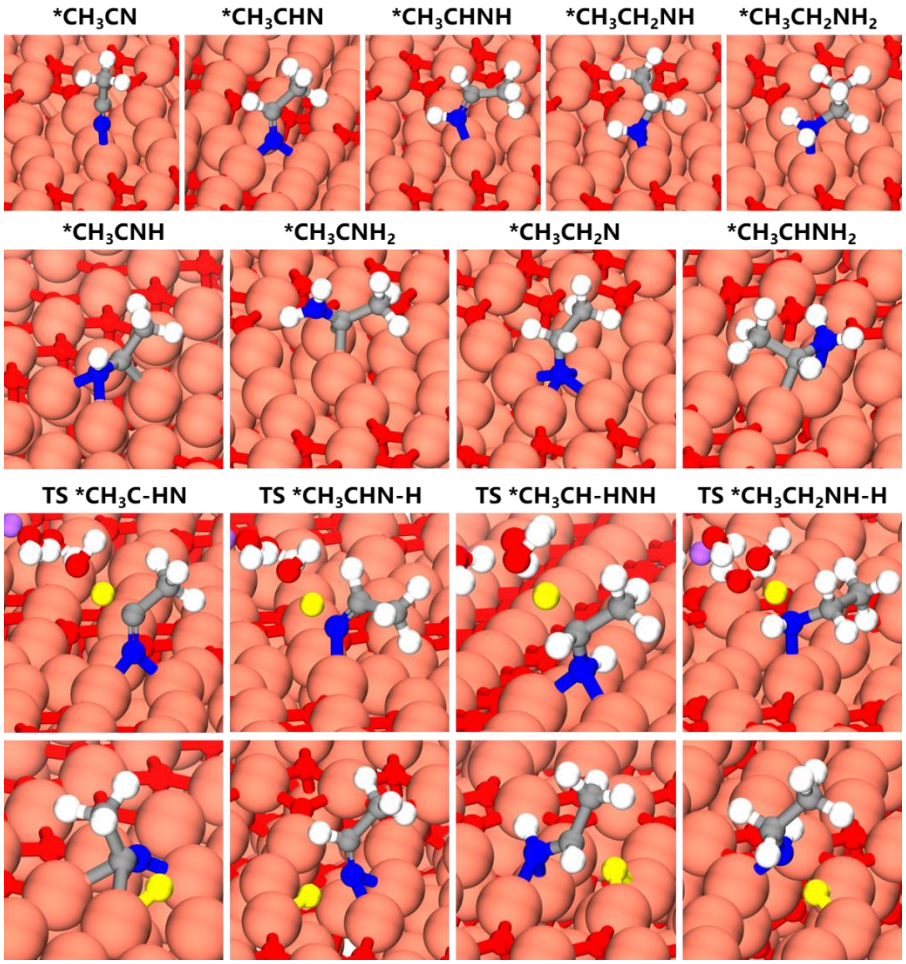

Figure S26. Optimized atomic structures of reaction intermediates and transition states involved in the ARR over CuO_x. The transferred hydrogen atoms in hydrogenation steps were highlighted.

Comment 6. Does this electrocatalytic hydrogenation method apply to other nitriles?

Reply: We have extended the electrocatalytic hydrogenation process to other nitriles, including butyronitrile, pentanenitrile, and cyclopropanecarbonitrile. For all these substrates, the selectivity towards the primary amine remains at 100%, with no detectable formation of secondary or tertiary amines. We have added the related discussion in the manuscript. The revision is as follows:

In Page 11 of the revised manuscript:

In additon we have extended the electrocatalytic hydrogenation process to other nitriles, including butyronitrile, cyclopropanecarbonitrile and pentanenitrile. For all these substrates, the selectivity towards the primary amine remains at 100%, with no detectable formation of secondary or tertiary amines (**Figure S19** and **Table S2**).

Table S2. Electrochemical hydrogenation of nitriles.

Entry	Nitrile	Primary amine	Selectivity (%)	FE (%)
1	cyclopropanecarbonitrile	cyclopropanemethylamine	100	81.5
2	butyronitrile	butylamine	100	66.0
3	pentanenitrile	pentylamine	100	53.6

The electrochemical hydrogen evolution reaction was performed in a 1 M NaOH aqueous solution containing nitrile (cyclopropanecarbonitrile and butyronitrile: 0.1 M, pentanenitrile: 0.2 M) in an H-type cell. The overall selectivity was evaluated by ^{1}H NMR spectroscopy, using TMS as the internal standard. The FE was evaluated based on the amount of H_2 generated, as determined by GC.

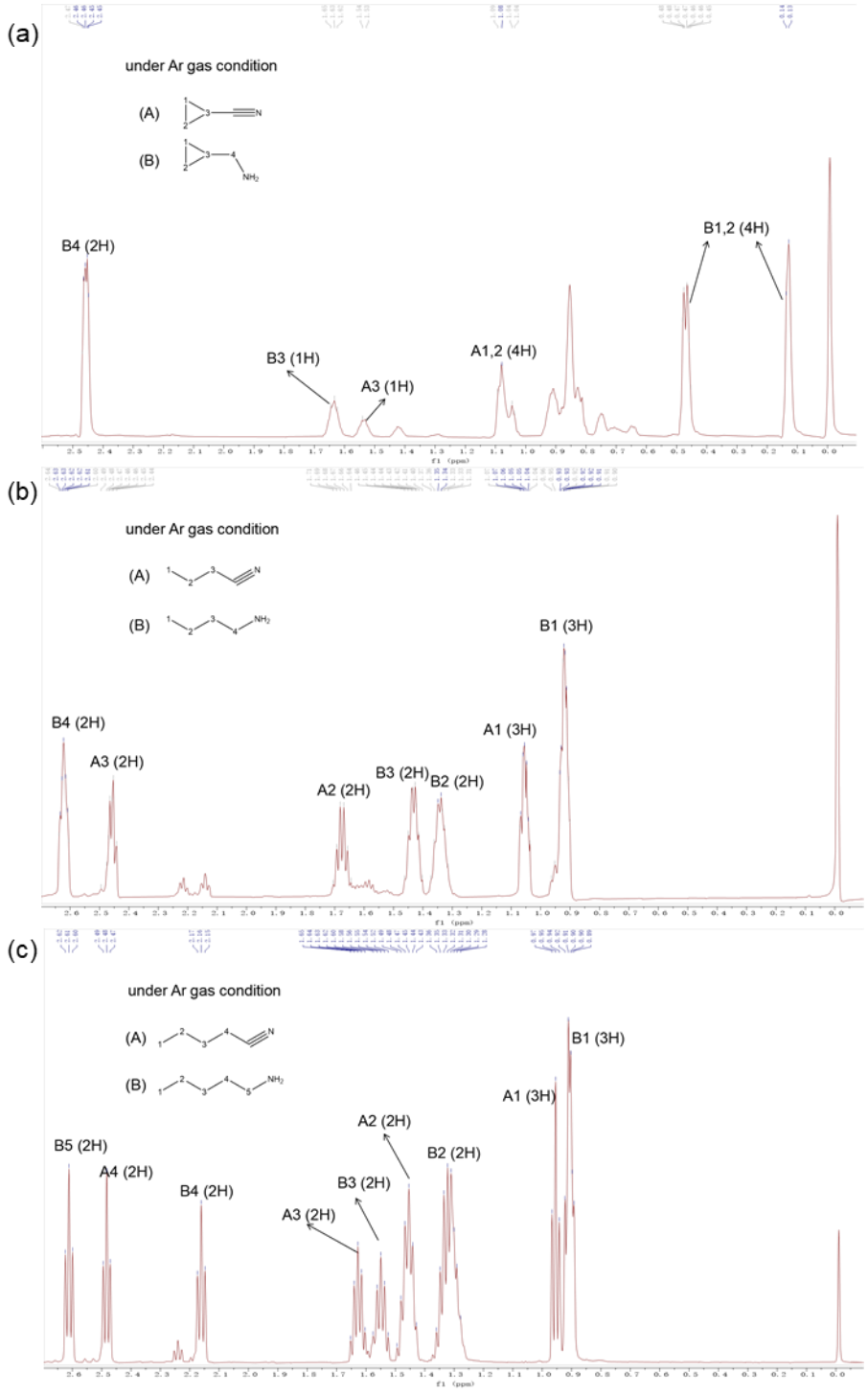

Figure S19. ^{1}H NMR spectrum of the liquid productss for the electrochemical hydrogenation of cyclopropanecarbonitrile (a), butyronitrile (b) and pentanenitrile (c).

Comment 7. In the references, the abbreviations and non abbreviations of magazine names are not unified, and references 5 and 24 are lacking. Reference 15 only gives the author's name, and other information is missing. Revise the non-conforming reference format of references according to the requirements of journals.

Reply: We have unified the references format, and added the missing information.

Comment 8. In the abstract and text, the abbreviation appearing for the first time should be marked with its full name.

Reply: Many thanks for your careful reading. We have revised it.

Reviewer #4 (Remarks to the Author):

This manuscript reported a synergistic hydrogenation process for the electroreduction of acetonitrile, which involves both surface hydrogen migration and proton addition from solution. The hydrogen evolution could be terminated at the Volmer step, and the protons migrate to the unsaturated bond of acetonitrile over a CuO@Cu heterostructure, thus significantly promoting the acetonitrile reduction process. This is an interesting finding with the impressive performance. The as-prepared CuO@Cu heterostructure exhibited outstanding stability for 1000 h at a large current density of 0.2 A cm^{-2}. I suggest its publication after suitable revisions.

Reply: We greatly appreciate the reviewer's positive comments and helpful suggestions. In response, we have revised the manuscript by providing additional explanations and discussions, as well as including new experiments and theoretical calculations to further strengthen our work.

Comment 1. The electroreduction reaction of acetonitrile to ethylamine has been investigated in 1M KOH solution only. How about the pH effect on ethylamine selectivity? For the long-term stability test in figure 2e, Nafion 117 was used as the membrane to separate cathode and anode in the electrolyzer. Since Nafion 117 is a proton exchange membrane, how stable is it in alkaline condition? Have authors employed an anion-exchange membrane in their electrolyzer?

Reply: We sincerely thank the reviewer for the raising the question regarding pH effect on ethylamine selectivity and the stability of Nafion 117.

In response to the pH effect on ethylamine selectivity, we investigate the ARR activity of the catalyst in several aqueous electrolyte solutions with varying pH values. The results are displayed in **Figure S9**. The ARR activity and the FE_{EA} of the catalyst increases with the concentration of NaOH in the electrolyte, indicating that a higher pH is favorable for the ARR process.

Regarding the reviewer's concerns on the stability of Nafion 117, we would like to emphasize that the Nafion 117 membrane is structurally stable under both acidic and alkaline conditions. In our study, we tried to use an anion exchange membrane (FAA-PK-130) in the liquid flow cell. However, due to its poor stability in the presence of acetonitrile, the membrane was easily damaged, as shown in **Figure R1** below. As a result, we switched to using the more stable Nafion 117 membrane to separate the anode and cathode. We agree that the Nafion 117 membrane may increase the local acidity on its surface which may influence the catalyst performance. However, since we did not assemble a membrane electrode system and the electrodes are self-supported, this configuration minimizes the impact of the membrane's local acidity. It is also worth noting that proton exchange membranes have been used in alkaline media in many studies [*Nat. Commun.*, 2021, 12, 1949; *Appl. Energy, 2019, 113323; J. Mater. Chem. A, 2022, 10, 13987-13997; J. Electroanal. Chem., 2022, 116680*]. We have added the related discussion in the manuscript.

In Page 6 of the revised manuscript: "To clarify the impact of pH on the electroreduction of acetonitrile, we investigate the ARR activity of the catalyst in several aqueous electrolyte solutions with varying pH values. The results are displayed in **Figure S9**. The ARR activity and the FE_{EA} of the catalyst increases with the concentration of NaOH in the electrolyte, indicating that a higher pH is favorable for the ARR process."

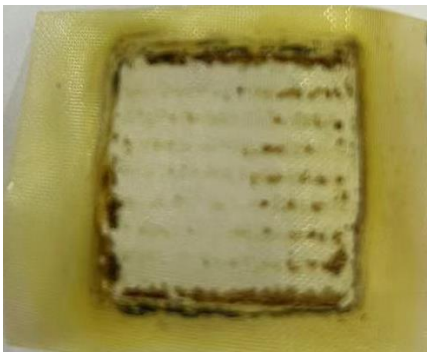

Figure R1. Photo of FAA-PK-130 after ARR test.

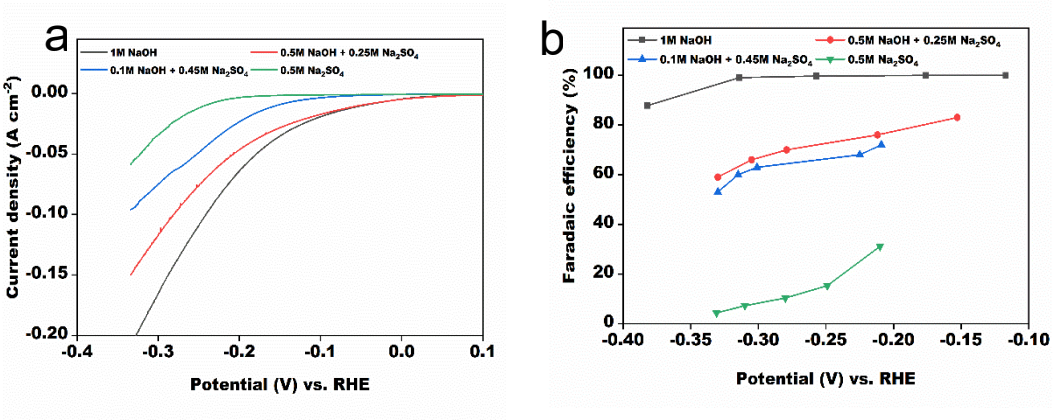

Figure S9. (a) LSV curves of CuO@Cu in different electrolyte; (b) the corresponding FEEA at different potentials.

Comment 2. The authors claimed that there are Cu^0, Cu^+ and Cu^{2+} oxidation states in the simulated CuO_x model according to the charge analysis. However, in Figure S13, only Cu^+ exists in Cu_2O (+0.53 |e|). Please comment on this.

Reply: We acknowledge that this expression is not very precise. The description has been revised as "According to the charge analysis, one can see that the Cu sites in the partially reduced surface are in various states, including Cu^0, $Cu^{\delta+}$ ($0 < \delta < 1$) and Cu^{2+} (**Figure S21**). "

In Page 12 of the revised manuscript: "According to the charge analysis, one can see that the Cu sites in the partially reduced surface are in various states, including Cu^0, $Cu^{\delta+}$ ($0 < \delta < 1$) and Cu^{2+} (**Figure S21**)."

Comment 3. In the computational details, authors indicated that the spin polarization was considered for CuO_x. Is the spin effect significant for these Cu-containing systems? The coordination environment and the side views of key reaction intermediates and transition states are highly suggested to be provided for reproduction.

Reply: The partially reduced CuO_x slab model possesses magnetic moment as 34.54, which increased to 34.63, 35.48, 35.22, 35.10 and 34.78 as $*CH_3CN$, $*CH_3CHN$,

*CH_3CHNH, *CH_3CH_2N and *$CH_3CH_2N_2$ adsorption, respectively. Considering the magnetic moments, the spin effect is supposed to impose significant effects on the energies of systems. The coordination environments and the side views of key reaction intermediates and transition states have been provided in **Figure S26** of the Supplementary Information.

In Page 5 of the revised Supplementary Materials: "For the CuO_x, spin polarization was considered due to its nonnegligible spin effects. A Hubbard correction of U = 5.0 eV was applied to the *d*-orbitals of Cu for better a description of the properties of Cu oxides [16, 17]."

In Page 32 of the revised Supplementary Information:

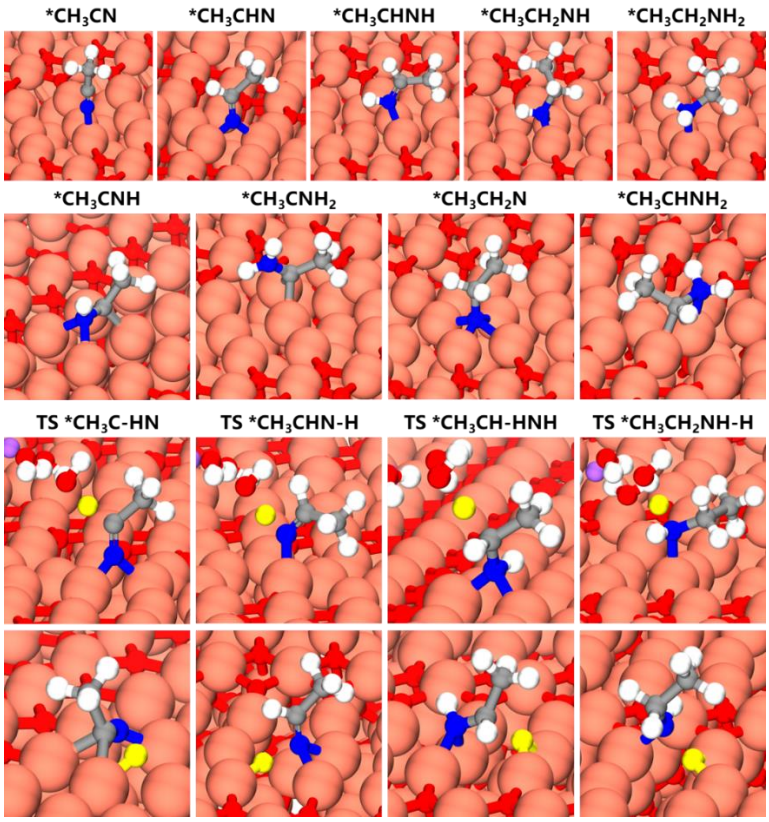

Figure S26. Optimized atomic structures of reaction intermediates and transition states involved in the ARR over CuO_x. The transferred hydrogen atoms in hydrogenation steps were highlighted.

Comment 4. The calibration curve should be provided for the reference electrode to prove the accuracy of the potential used in the study.

Reply: We have added the calibration curve in Supplementary Material.

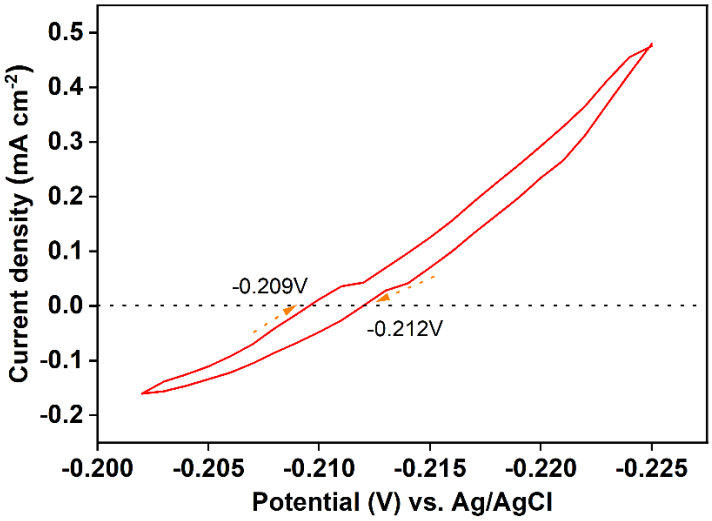

Figure S3. Calibration test for Ag/AgCl reference electrode.

Comment 5. Cuprous oxide nanoparticles should be added as a control sample to compare with the CuO@Cu heterostructure for acetonitrile reduction.

Reply: Many thanks for your helpful suggestion. The ARR performance of CuO nanoparticles has been provided. As shown in **Figure S6**, CuO@Cu heterostructure exhibits much higher ARR activity than that of CuO nanoparticles. The revision is as follows:

In Page 7 of the revised manuscript: "As shown in **Figure S6**, CuO@Cu heterostructure exhibits much higher ARR activity than that of CuO nanoparticles."

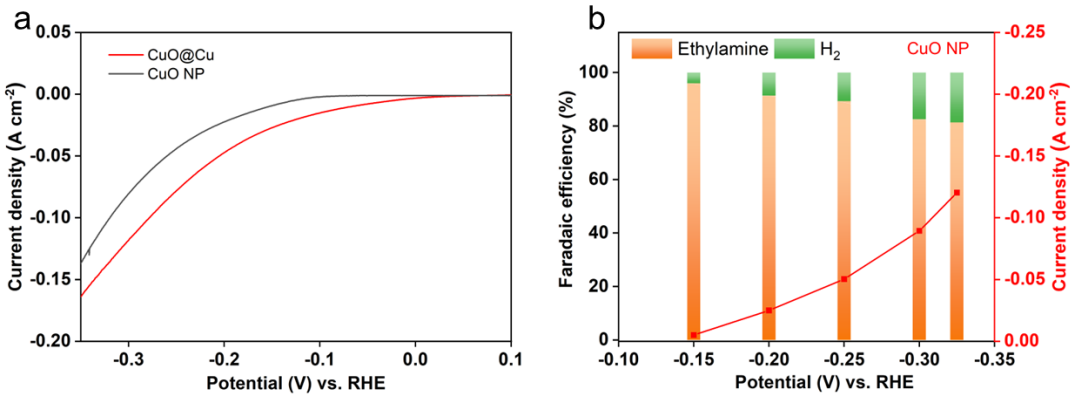

Figure S6. (a) LSV curves of CuO@Cu and CuO NP in 1 M NaOH solution with acetonitrile; (b) FE_{EA} at different potentials in CuO NP.

Comment 6. An irrelevant horizontal line was observed in Figure 1. Please check and correct.

Reply: We appreciate the reviewer for your careful reading. We have removed horizontal line in the **Figure 1**.